The stoichiometry of the *Escherichia coli* Hfq protein bound to RNA

TAYLOR B. UPDEGROVE,[1,2] JOHN J. CORREIA,[3] YANFENG CHEN,[2] CHARLES TERRY,[1,2] and ROGER M. WARTELL[1,2]

[1]School of Biology, Georgia Institute of Technology, Atlanta, Georgia 30332, USA
[2]Parker H. Petit Institute for Bioscience and Bioengineering, Georgia Institute of Technology, Atlanta, Georgia 30332, USA
[3]Department of Biochemistry, University of Mississippi Medical Center, Jackson, Mississippi 39216, USA

ABSTRACT

The *Escherichia coli* RNA binding protein Hfq is involved in many aspects of post-transcriptional gene expression. Tight binding of Hfq to polyadenylate sequences at the 3′ end of mRNAs influences exonucleolytic degradation, while Hfq binding to small noncoding RNAs (sRNA) and their targeted mRNAs facilitate their hybridization which in turn effects translation. Hfq binding to an A-rich tract in the 5′ leader region of the *rpoS* mRNA and to the sRNA DsrA have been shown to be important for DsrA enhanced translation initiation of this mRNA. The complexes of Hfq-A_{18} and Hfq-DsrA provide models for understanding how Hfq interacts with these two RNA sequence/structure motifs. Different methods have reported different values for the stoichiometry of Hfq-A_{18} and Hfq-DsrA. In this work, mass spectrometry and analytical ultracentrifugation provide direct evidence that the strong binding mode of the Hfq hexamer (Hfq_6) for A_{18} and domain II of DsrA ($DsrA_{DII}$) involve 1:1 complexes. This stoichiometry was also supported by fluorescence anisotropy and a competition gel mobility shift experiment using wild-type and truncated Hfq. More limited studies of Hfq binding to DsrA as well as to the sRNAs RprA, OxyS, and an 18-nt segment of OxyS were also consistent with 1:1 stoichiometry. Mass spectrometry of cross-linked samples of Hfq_6, A_{18}, and $DsrA_{DII}$ exhibit intensity corresponding to a ternary 1:1:1 complex; however, the small intensity of this peak and fluorescence anisotropy experiments did not provide evidence that this ternary complex is stable in solution.

Keywords: Hfq; DsrA; RprA; OxyS; MALDI-TOF

INTRODUCTION

The Hfq protein of *Escherichia coli* is a RNA binding protein and a key factor in post-transcriptional gene regulation (Valentin-Hansen et al. 2004; Majdalani et al. 2005; Brennan and Link 2007; Waters and Storz 2009). *E. coli* Hfq and its bacterial homologs have been implicated in various facets of bacterial metabolism, including stress-induced sRNA regulation of mRNA translation as well as mRNA stability. In addition to its well-documented interaction with RNA, Hfq has been found associated with DNA (Takada et al. 1997; Azam et al. 2000; Updegrove et al. 2010) as well as a number of proteins (Butland et al. 2005). The nature of Hfq's interactions with DNA and many of the proteins are not well understood; however, there is increasing recognition that they may reflect additional functions of Hfq (Le Derout et al. 2010).

Considerable attention has been focused on the role of Hfq in gene regulation by noncoding small RNAs (sRNAs). A number of sRNAs, such as OxyS, SgrS, DsrA, RprA, Spot42, and Qrr1-4, require Hfq to facilitate their regulation of mRNA translation (Sledjeski et al. 2001; Majdalani et al. 2002; Moller et al. 2002a,b; Zhang et al. 2002; Lenz et al. 2004; Kawamoto et al. 2006). In vitro studies suggest that Hfq's role is to enhance the association rate and/or stability of a sRNA to its mRNA target site near the start codon (Geissmann and Touati 2004; Kawamoto et al. 2006; Soper and Woodson 2008; Updegrove et al. 2008). The formation of a sRNA–mRNA hybrid can inhibit or enhance ribosome accessibility to mRNA, thus providing either negative or positive regulation of translation (Majdalani et al. 2005; Waters and Storz 2009). Hfq's presence in the cell enhances sRNA stability and its capacity for functional interaction with mRNA targets. Hfq has also been shown to influence mRNA stability in vivo by enhancing sRNA–mRNA

Reprint requests to: Roger M. Wartell, School of Biology, Georgia Institute of Technology, Atlanta, Georgia 30332, USA; e-mail: roger.wartell@biology.gatech.edu; fax: (404) 894-0519.

Article published online ahead of print. Article and publication date are at http://www.rnajournal.org/cgi/doi/10.1261/rna.2452111.

interaction or by binding mRNA directly (Tsui et al. 1997; Vytvytska et al. 1998; Masse et al. 2003; Morita et al. 2005).

In addition to its interactions with the translational initiation regions of mRNAs, Hfq also influences the stability of some mRNAs through its interaction with their 3′ ends. It has been estimated that >90% of the *E. coli* transcriptome possess post-transcriptionally added poly(A) tails (Mohanty and Kushner 2006). Studies show that Hfq stimulates the addition of poly(A) tails to the 3′ end of some mRNAs by poly(A) polymerase I (PAP) (Le Derout et al. 2003; Mohanty et al. 2004; Folichon et al. 2005). In vivo, inactivation of the *hfq* gene reduces the length of poly(A) tails synthesized at the 3′ end of the *rpsO* mRNA by PAP, and in vitro, the addition of Hfq increases the processivity of PAP on *rpsO* mRNA. The addition of poly(A) tails has been shown to enhance mRNA decay in eubacteria (Steege 2000). Studies also indicate that Hfq binding to poly(A) tails can prevent mRNAs from binding to enzymes involved in RNA degradation (Folichon et al. 2003, 2005; Mohanty et al. 2004). Understanding the role of Hfq in the degradation of mRNAs requires understanding how Hfq binds to the 3′ ends of mRNAs with poly(A) tails, as well as with PAP and possibly other RNA processing enzymes.

Initial studies on Hfq binding to RNA homopolymers and oligomers demonstrated that Hfq has a strong affinity for poly(A) and A_n oligomers with $n > 15$ (Carmichael et al. 1975; de Haseth and Uhlenbeck 1980b). Studies on the binding of mutant Hfq to A_n oligomers indicated that the distal surface of the Hfq hexamer (Hfq_6) interacts with poly(A) sequences (Mikulecky et al. 2004; Sun and Wartell 2006). A binding model proposed to accommodate information on the complex (Brennan and Link 2007), and a recent crystal structure of *E. coli* Hfq and A_{15} imply that the Hfq_6 forms a 1:1 complex with A_n oligomers. However, experimental studies employing several methodologies suggested different stoichiometries for Hfq and oligoriboadenylates. Isothermal titration calorimetry suggested one Hfq_6 bound to two A_{18} (Mikulecky et al. 2004), while fluorescence anisotropy, fluorescence quenching and a gel shift assay supported a model in which two Hfq_6 was bound to one A_{18} (Sun and Wartell 2006).

DsrA is an 87-nucleotide (nt) sRNA that acts as a positive regulator for the translation of the stationary phase sigma factor RpoS. Hfq facilitates DsrA binding to the leader region of the *rpoS* mRNA and releases an inhibitory stem–loop that sequesters the Shine-Delgarno (SD) sequence (Cunning et al. 1998). Hfq binds both DsrA and *rpoS* mRNA with similar affinities (Soper and Woodson 2008; Updegrove et al. 2008). Studies have explored the number of Hfq molecules binding to each RNA participant. Gel shift measurements yielded data supporting a 2:1 (Hfq_6:RNA) binding model for a 138-nt segment of *rpoS* mRNA, DsrA (Lease and Woodson 2004), and $DsrA_{DII}$ (Sun and Wartell 2006), while isothermal titration calorimetry indicated a 1:1 complex for Hfq_6 binding to DsrA and a segment of *rpoS* mRNA (Mikulecky et al. 2004).

The ability of Hfq to stimulate sRNA–mRNA duplex formation has been observed under both in vitro and in vivo conditions. How Hfq recognizes and binds each of the RNAs and facilitates their pairing remains obscure. Evidence that Hfq can alter secondary and/or tertiary structure of some sRNAs and mRNAs lends support to the notion that Hfq acts as a chaperone and modulates the sRNA and/or mRNA structure, making one or the other RNA more amendable for heteroduplex formation. Another role ascribed to Hfq is an ability to bind and hold two pairing RNA molecules simultaneously, thus bringing them in close proximity and driving the reaction to favor sRNA–mRNA duplex formation. However, we note that the ability of Hfq to separately bind two complementary RNAs is not always sufficient to promote RNA pairing (Arluison et al. 2007). Exactly how Hfq brings together two independent RNA molecules depends on the number of Hfq hexamers required to bind each RNA molecule and the number and type of RNAs that can simultaneously bind each Hfq hexamer. The stoichiometry of Hfq_6 binding to RNA is clearly pertinent to understanding the mechanism of how Hfq promotes ribo-regulation.

The focus of the current work was to determine the stoichiometry of the strong binding complexes of Hfq with A_{18} and $DsrA_{DII}$. The oligoriboadenylate A_{18} mimics the size and sequence of poly(A) tails at the 3′ end of mRNAs, and results on how this oligonucleotide interacts with Hfq may be of functional significance in terms of Hfq's role and mechanism in facilitating polyadenylation by poly(A) polymerase. $DsrA_{DII}$, a 38-nt portion of DsrA (nucleotides 23–60), competes with DsrA for binding to Hfq (Brescia et al. 2003). It contains a stem–loop and U-rich segment of DsrA that binds Hfq. Mass spectrometry, fluorescence anisotropy, and analytical ultracentrifugation provide evidence supporting a 1:1 stoichiometry for Hfq_6 and oligo A_{18} as well as for Hfq_6 and $DsrA_{DII}$. A competition electrophoretic gel mobility shift assay also supports 1:1 complexes for Hfq_6 binding to A_{18} as well as to full-length DsrA, RprA, and OxyS.

RESULTS

MALDI-TOF mass spectroscopy indicates Hfq_6 forms a 1:1 complex with $DsrA_{DII}$, A_{18}, and OxyS-18

MALDI-TOF (matrix-assisted laser desorption ionization-time of flight) mass spectrometry was first used to examine the molecular mass of *E. coli* Hfq alone and then as a complex with A_{18}. These experiments were done in the absence of cross-linking as well as after EDC cross-linking of the Hfq-A_{18} complex prior to mass spectrometric analysis. The MALDI-TOF spectrum of Hfq shown in Figure 1a was carried out with EDC cross-linking and reveals discrete ions

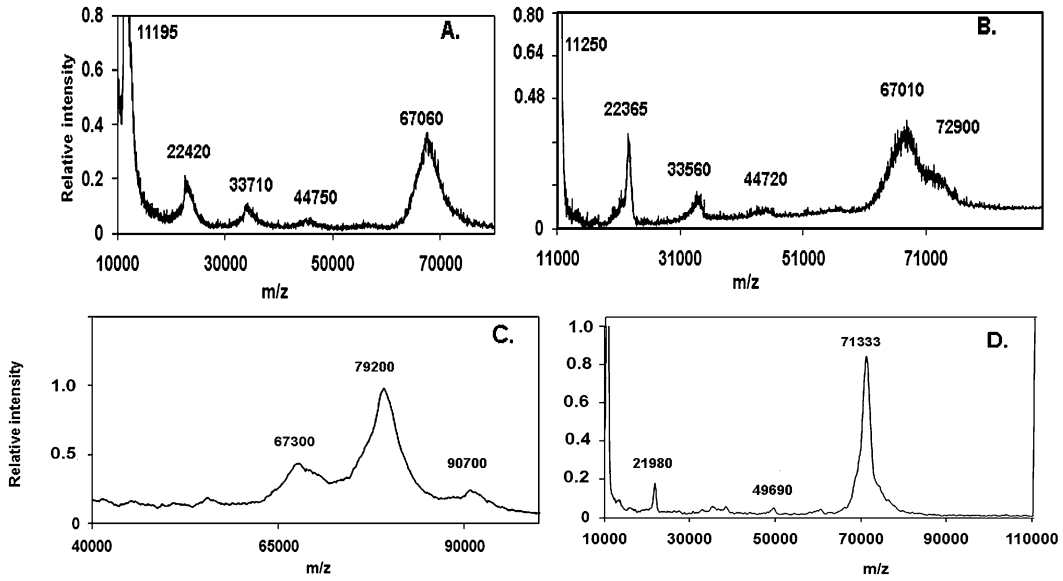

FIGURE 1. MALDI-TOF m/z spectra of 2 μM Hfq_6 (*A*), 2 μM Hfq_6 and 0.7 μM A_{18} (*B*), 8 μM Hfq_6 and 4 μM DsrA domain II (*C*), and 4 μM Hfq_6 and 2 μM OxyS-18 (*D*). All samples were prepared in the 0.2 M Na^+ solvent and matrix solution as described in Materials and Methods.

with m/z ratios corresponding to the Hfq monomer and multimers up to the hexamer (67,060 Da; theoretical mass, 66,998 Da). This observation is in agreement with a previous study (Moller et al. 2002a) and illustrates that Hfq can stably exist as multimers up to the hexamer in the laser desorption ionization process. We note that macromolecules are generally expected to be singly charged ions in MALDI-TOF experiments (Karas et al. 2000).

The addition of 0.7 μM A_{18} to 2 μM Hfq_6 resulted in the formation of an additional peak corresponding to a molecular mass of 72,900 Da (Fig. 1b). Since the theoretical mass of A_{18} is 5,840 Da, this new peak is very close to an expected complex with a 1:1 ratio of Hfq_6 to A_{18} (theoretical mass, 72,839 Da). No peaks were observed at the molecular mass corresponding to 2:1 or 1:2 ratios of Hfq_6 to A_{18}. Similar results were also obtained when 0.07 μM A_{18} and 0.2 μM Hfq_6 were employed with and without EDC cross-linking (data not shown). The addition of EDC increased the relative signal intensities of the Hfq_6 and Hfq_6•A_{18} complex over the Hfq subunit multimers, consistent with suppression of hexamer dissociation.

The Hfq_6–$DsrA_{DII}$ complex required a more robust cross-linking agent to withstand the conditions imposed by the MALDI-TOF experiment. Formaldehyde proved to be an efficient cross-linker and allowed detection of the Hfq_6–$DsrA_{DII}$ complex. Figure 1c shows a spectrum resulting from a mixture of 8 μM Hfq_6 with 4 μM $DsrA_{DII}$. A pronounced peak occurs at a m/z ratio of 79,200 flanked by less pronounced peaks of 67,300 and 90,700. Since the theoretical molecular weight of $DsrA_{DII}$ is 12,031 Da, the large middle peak is consistent with one Hfq_6 bound to one $DsrA_{DII}$. The smaller and larger molecular weight peaks are consistent with Hfq_6 and one Hfq_6 bound to two $DsrA_{DII}$ molecules, respectively. $DsrA_{DII}$ has been shown to form two bands at low μM concentrations in a polyacrylamide gel environment (Sun and Wartell 2006). When 2 μM Hfq_6 was added to 1 μM $DsrA_{DII}$, only the 79,000 and 67,000 m/z peaks were observed (data not shown). Unfortunately a MALDI-TOF experiment with full-length DsrA and Hfq gave weak or negligible signals barely above background at the m/z ratio expected for Hfq_6•DsrA or higher masses. The larger negative charge intrinsic to the full-length DsrA molecule appears to compromise a study of this complex by this method.

OxyS is a 109-nt sRNA that was shown to bind Hfq in vitro and in vivo and acts as a negative regulator for the translation of the *rpoS* mRNA. A 18-nt portion of OxyS sRNA that spans nucleotides 64–81 is thought to be critical for Hfq binding based on the observation that an oligonucleotide complementary to this region strongly inhibits Hfq from binding to the full-length OxyS molecule (Zhang et al. 2002). MALDI-TOF was used to assess the stoichiometry of Hfq binding to this segment of OxyS. When 4 μM of Hfq_6 was added to 2 μM OxyS-18 and formaldehyde is used as the cross-linking agent, only one extremely large peak was observed at an m/z ratio of 71333 (Fig. 1d). With the theoretical molecular weight of OxyS-18 being 5769.6 Da, the large peak in Figure 1d is in good agreement with one Hfq hexamer bound to one OxyS-18. No peak was detected at an m/z ratio corresponding to either 1:2 or 2:1 Hfq_6 to OxyS-18 stoichiometry.

Analytical ultracentrifugation analysis of Hfq•A_{18} complex in solution

Analytical ultracentrifugation analysis was employed to determine the stoichiometry of the Hfq-A_{18} complex in aqueous solution. Sedimentation velocity of Hfq alone in

0.5 M NaCl and 20 mM Tris (8.2) indicated a single major species with a sedimentation coefficient (*s*) of *s* = 3.42 sec <3.41, 3.44> and no more than 2% of a higher molecular weight aggregate with *s* = 5.56 S. Figure 2a shows the results of a sedimentation velocity experiment of Hfq analyzed using the c(*s*) method (Schuck et al. 2002). The sedimentation coefficient distribution was independent of loading concentrations from 3.2–12.1 μM Hfq in moles hexamer. Direct boundary fitting of the sedimentation velocity data using SedAnal (Stafford and Sherwood 2004) indicated a molecular weight for the 3.42 S species of 64,815 Da <59,733, 70,301>. This value is slightly lower than the expected value of 66,998 Da and is consistent with the hexamer being the dominant Hfq species at these concentrations. The slightly lower than expected value can be explained by uncertainty in the partial specific volume employed or the influence of the minor aggregate on the fit. (Traces of sediment velocity run and model fitting using SedAnal are given in Supplemental Fig. S1.)

Figure 2b shows the normalized g(*s*) distribution of concurrently run sedimentation velocity experiments which examined 6.9 μM Hfq_6 alone, 6.9 μM Hfq_6 with 4.4 μM FAM-A_{18}, and 6.9 μM Hfq_6 with 8.3 μM FAM-A_{18}. FAM-A_{18} binding increased the sedimentation coefficient of Hfq_6 from 3.3S to 3.9S. At the concentration ratio of [FAM-A_{18}]/[Hfq_6] of 1.2, a trailing boundary of excess FAM-A_{18} is observed. Free FAM-A_{18} has a sedimentation coefficient of 1.355 S <1.345, 1.364> with no evidence of concentration dependence or additional species (data not shown). Using the SedAnal software, a good fit to the Hfq-A_{18} data was obtained with a model that assumed Hfq hexamer binds A_{18} with a 1:1 stoichiometry. The best Sedanal fit (constraining S for Hfq and FAM-A_{18}) returned a K of 1.71×10^7 M^{-1} <0.85, UB>. The unbounded upper limit means all larger values of K are indistinguishable in the least-squares sense. A subsequent run with a new protein sample returned a larger K $\sim 10^{10}$ M^{-1} with 95% confidence limits of $<7.5 \times 10^7$, UB>. Thus the data is consistent with a tight 1:1 Hfq-A_{18} complex with an affinity in excess of $10^7 M^{-1}$.

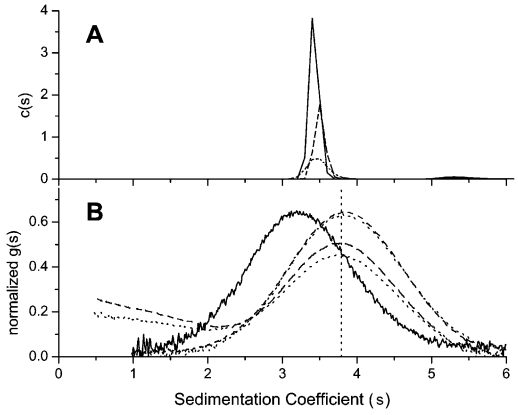

FIGURE 2. (*A*) Sedimentation coefficient distribution c(*s*) determined by program Sedfit for three different Hfq_6 concentrations, 3.2, 5.7, and 12 μM shown as dotted, dashed, and solid lines, respectively. The average integrated value for these data is 3.51 ± 0.03 S. (*B*) Sedimentation coefficient distribution displayed as normalized g(*s*) for Hfq_6 at 6.9 μM alone as solid line (average integrated value for Hfq data is 3.42 ± 0.04 S), and with 4.4 μM and 8.3 μM FAM-A_{18} added. Upper pair of overlapping dashed and dotted lines show the 6.9:4.4 mixture evaluated by absorbance at 274 nm and 495 nm, respectively. Lower pair of dashed and dotted lines display the 6.9:8.3 mixture evaluated at the same two wavelengths. Lack of alignment of c(*s*) and g(*s*) peaks for Hfq_6 alone (3.51 S vs. 3.42 S) is attributed to minor components affecting the main c(*s*) peak.

Sedimentation equilibrium runs of 2, 4, and 8 μM Hfq_6 alone and mixed with 1:1 molar ratios of FAM-A_{18} confirmed that the stoichiometry of the Hfq_6•FAM-A_{18} complex in solution is not 2:1, but 1:1. The evaluated molecular weight of Hfq alone was 61.475 kDa <58.8, 64.2> (rms = 0.00596) (Supplemental Fig. S2), similar to the value obtained from sedimentation velocity analysis. Analysis of the sedimentation equilibrium data of the Hfq•FAM-A_{18} mixtures, monitored at the FAM-A_{18} absorbance peak of 495 nm, yielded a molecular weight of 68.93 kDa <67.4, 70.4> (rms = 0.00724) (Supplemental Fig. S2). This clearly does not correspond to a complex consisting of 2 Hfq_6 molecules and one A_{18} molecule but is consistent with a 1:1 complex.

Gel mobility shift study of wild-type Hfq and Hfq-65 binding to A_{18} and other RNAs

Previous gel mobility experiments in which A_{18} or other RNAs were titrated with Hfq at concentrations above apparent K_d values indicated 2:1 Hfq_6 to RNA stoichiometry (Lease and Woodson 2004; Sun and Wartell 2006; Updegrove et al. 2008) . Since these previous results conflict with the above findings, we examined the stoichiometry of Hfq•A_{18} complexes in the gel environment using a different approach that relies on a qualitative comparison rather than quantative analysis of band intensities. The Hfq•A_{18} complexes that formed in the presence of wild-type (wt) Hfq and Hfq-65 were determined. Hfq-65 is a truncated variant of wt Hfq consisting of 65 residues from the N-terminal end. This truncated Hfq was previously shown to bind DsrA two- to threefold less well than wt Hfq, and to A_{27} with an affinity similar to wt Hfq (Vecerek et al. 2008). Lane 3 of Figure 3a shows the gel-shift of the Hfq-65•A_{18} complex in a 6% PAG. The Hfq-65•A_{18} complex migrates with a slower mobility than the wt Hfq•A_{18} complex (lane 2) in spite of its reduced size. A plausible explanation of this phenomenon is the increased positive charge of Hfq-65 compared to wt Hfq. Hfq-65 has four less negatively charged residues (Asp 97, Glu 99, Glu 100, and Glu 102) and one less positively charged residue (Arg 66) than each wt Hfq subunit. When equimolar amounts of wt Hfq and Hfq-65 were mixed with A_{18} for 5 min and run into the gel, two bands were observed corresponding to wt Hfq•A_{18}

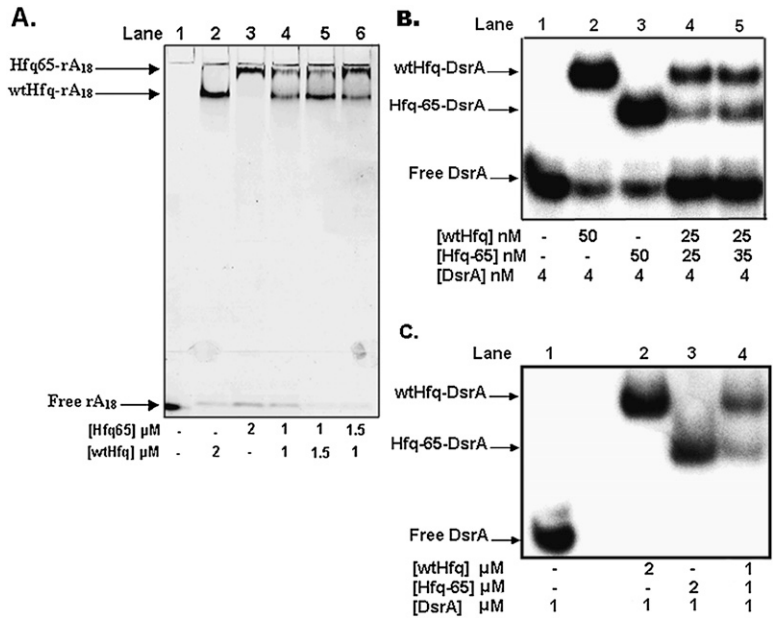

FIGURE 3. DsrA and A$_{18}$ bind both wt Hfq and Hfq-65 in a 1:1 stoichiometry. Varying concentrations in moles hexamer/L of wt Hfq and Hfq-65 were added to 1 µM FAM-A$_{18}$ (*A*), 4 nM ^{32}P-DsrA (*B*), and 1 µM ^{32}P-DsrA (*C*). Similar results were obtained when ^{32}P end-labeled RprA and OxyS sRNAs were added to both wt Hfq and Hfq-65.

and Hfq-65•A$_{18}$ (Fig. 3a, lane 4). This result is consistent with a 1:1 stoichiometry for complexes of Hfq$_6$ and A$_{18}$. If the stoichiometry of the Hfq•A$_{18}$ complexes were two Hfq$_6$ and one A$_{18}$, a band of intermediate mobility would be expected in lane 4. Changing the ratio of wt Hfq and Hfq-65 concentrations altered the intensity of the two bands in direct proportion, but no additional band is observed (Fig. 3a, lanes 5,6).

When 4 nM ^{32}P-labeled DsrA was added to 50 nM of either wt Hfq or Hfq-65 (moles hexamer), most of the RNA was shifted to a slower moving complex. Under these conditions, the DsrA•Hfq-65 complex migrates faster than the DsrA•wt Hfq complex (Fig. 3b, lanes 2,3). Since DsrA has considerably more negative charge than A$_{18}$, it will likely dominate the charge differences between wt Hfq and Hfq-65. The size difference between wt Hfq and Hfq-65, rather than their intrinsic charge difference, appears to be the governing factor in the migration of these Hfq•DsrA complexes. When 25 nM wt Hfq and 25 nM Hfq-65 (moles hexamer) were added to 4 nM DsrA, only two apparent slow migrating bands were evident; one corresponding to the DsrA•wt Hfq complex and the other corresponding to the DsrA•Hfq-65 complex (Fig. 3b, lane 4). Similarly, when 1 µM each of wt Hfq and Hfq-65 was added to 1 µM DsrA, only two slow migrating bands were observed (Fig. 3c, lane 4). The outcome was the same when 25 nM wt Hfq and 25 nM Hfq-65 was added to 4 nM ^{32}P-labeled OxyS or RprA (data not shown). The results are consistent with a 1:1 stoichiometry for Hfq$_6$ binding to these RNAs.

Hfq binding to A$_{18}$ or DsrA$_{DII}$ monitored by fluorescence anisotropy.

Another experimental approach that suggested two Hfq$_6$ bound A$_{18}$ was fluorescence anisotropy (Sun and Wartell 2006). A model in which two Hfq$_6$ sequentially bound A$_{18}$ gave a better fit to fluorescence anisotropy data than a model that assumed a 1:1 complex. We have re-examined and extended these measurements and the analyses in light of the above results. Figure 4a shows that the 2:1 binding model (solid line) does give the best fit to the titration of Hfq to 2 nM of FAM-labeled A$_{18}$. The dotted line is the nonlinear least-squares fit of the 1:1 model (Equation 1 in the Materials and Methods), with K$_d$ a variable parameter and the other parameters (A_f, A_b, $[R]_T$, $[P]_T$) determined from the experimental data. The A_b value of 0.166 was determined from the horizontal asymptote to the anisotropy values of the four highest Hfq$_6$ concentrations used in the experiment. If, however, one allows A_b to be somewhat flexible and assume a value of 0.185, the fit of the 1:1 model approaches that of the 2:1 model (dashed line). Considering that the 2:1 model has more variable parameters with which to fit the data, the difference between the two models no longer persuasively favors the 2:1 model. Both models indicate K$_d$ values in the range of 5–10 nM.

To further examine the stoichiometry of Hfq$_6$ binding to A$_{18}$ using this experimental approach, the titration of A$_{18}$ with Hfq was carried out at concentrations well above the K$_d$ (5 µM A$_{18}$) where stoichiometric binding is expected. Figure 4b shows that the anisotropy change of A$_{18}$ saturates at a ratio of Hfq$_6$ and A$_{18}$ consistent with a 1:1 stoichiometry. A similar experiment conducted with 2 µM DsrA$_{DII}$ also showed a break in the plot at a 1:1 molar ratio of Hfq$_6$ and DsrA$_{DII}$ (Fig. 4c). The K$_d$ of Hfq$_6$ binding to DsrA$_{DII}$ under the conditions of the experiment (0.1 M NaCl + 20 mM Tris) was ~4 nM (Supplemental Fig. S3).

Hfq interaction with both A$_{18}$ and DsrA$_{DII}$

Polyacrylamide gel mobility shift experiments have previously demonstrated that Hfq can form a complex with a poly(A) sequence and DsrA (Brescia et al. 2003). The observation of a "super shifted" gel band consisting of the above three components indicates a ternary complex but does not exclude the possibility that more than one Hfq hexamer is needed to form this complex. MALDI-TOF mass spectrometry was employed to examine if a mass could be

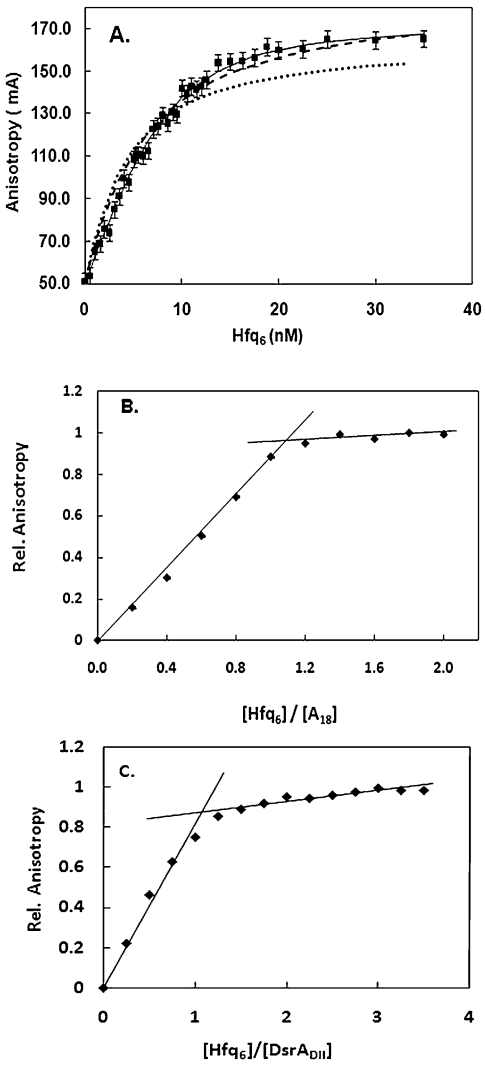

FIGURE 4. Fluorescence anisotropy titration of FAM-A_{18} with Hfq. (*A*) Comparison of experimental data with 2 nM FAM-A_{18} (squares) to best fit of 2:1 model (solid line), 1:1 model with K_d variable (circles), and 1:1 model with variable K_d and A_b (dotted line). Parameters for: 2:1 model; K_1 = 10.1 nM, K_2 = 5 nM, A_{b1} = 0.148, A_{b2} = 0.172. For 1:1 models; K_1 = 4.4 nM, A_b = 0.166 for dotted line, K_1 = 5 nM, A_b = 0.185 for dashed line. (*B*) Experimental anisotropy measurements of 5 μM FAM-A_{18} titrated with Hfq_6. (*C*) Experimental anisotropy measurements of 2 μM $DsrA_{DII}$ titrated with Hfq_6.

detected consistent with a complex formed by Hfq_6, $DsrA_{DII}$, and A_{18}. We mixed 10 μM Hfq_6 with 5 μM $DsrA_{DII}$ and 5 μM A_{18} for 15 min, which was treated with formaldehyde as described in Materials and Methods. Figure 5 shows the MALDI-TOF spectrum of this sample. Peaks were observed corresponding to molecular masses very similar to Hfq_6 (66,650 Da; theoretical mass, 66,998 Da), Hfq_6•A_{18} (72,400 Da; theoretical mass, 72,839 Da), and Hfq_6•$DsrA_{DII}$ (78,230 Da; theoretical mass, 79,029 Da). A small but reproducible peak was observed in the region corresponding to a mass of 84,355 Da, consistent with the combined mass of one Hfq_6, one A_{18}, and one $DsrA_{DII}$ (theoretical mass, 84,869 Da). We note that the lower observed masses compared to theoretical masses (by 350–700 Da) appears to be due to external calibration error.

The small peak corresponding to a mass of 55,530 Da is consistent with five subunits of Hfq (theoretical mass, 55,832 Da). Small nearby peaks were reproducibly observed and may be related to four or five subunits of Hfq with A_{18}, $DsrA_{DII}$, or both. The intensities of peaks corresponding to the unbound forms of four and five Hfq subunits were slightly higher (relative to the Hfq monomer peak) in the presence of both $DsrA_{DII}$ and A_{18} (~3%) compared to when only one RNA was present (~2%). Not surprisingly, the Hfq•A_{18} and Hfq•$DsrA_{DII}$ peaks were smaller by about 2.5-fold when both $DsrA_{DII}$ and A_{18} were present compared with spectra of Hfq and only one RNA. The small peak at 89,515 is consistent with one Hfq_6 and a dimer of $DsrA_{DII}$ and is similar to the small peak observed with Hfq and $DsrA_{DII}$ (Fig. 1c).

The intensity in the region of the 84,355 Da mass in Figure 5 is consistent with a 1:1:1 Hfq_6•A_{18}•$DsrA_{DII}$ ternary complex; however, this peak was considerably smaller than the peaks corresponding to Hfq_6•A_{18} or Hfq_6•$DsrA_{DII}$. This may reflect an intrinsic instability of this ternary complex or a limitation of the method in reporting complexes of Hfq_6 with two RNAs.

To explore this question in solution, we examined the effect of adding $DsrA_{DII}$ on the fluorescence anisotropy of a preformed complex of Hfq_6•FAM-A_{18}. Hfq_6 was added to 100 nM FAM-A_{18} in a solvent of 0.1 M NaCl+ 20 mM Tris (8.3), increasing the anisotropy from 0.037 to 0.080, about 45% of the maximum anisotropy change induced by saturating Hfq_6. Adding aliquots of $DsrA_{DII}$ to produce a final solution with 75 nM FAM-A_{18}, 65 nM $DsrA_{DII}$, and 63 nM Hfq_6 reduced the anisotropy by about 30% (Fig. 6). If a ternary Hfq_6•A_{18}•$DsrA_{DII}$ complex is stable relative to the 1:1 Hfq_6•RNA complexes, an increase rather than decrease in anisotropy is expected. This experiment was repeated using the complete DsrA, surmising its higher molecular weight and strong binding to Hfq_6 may be required to

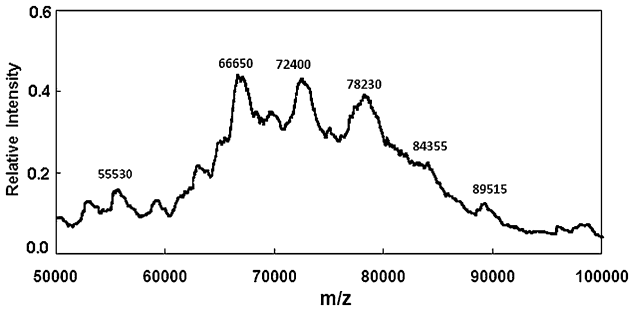

FIGURE 5. MALDI-TOF m/z spectrum of 10 μM Hfq_6 plus 5 μM $DsrA_{DII}$ and 5 μM A_{18} prepared in the 0.2 M Na^+ solvent, cross-linked with formaldehyde, and mixed with matrix solution as described in Material and Methods.

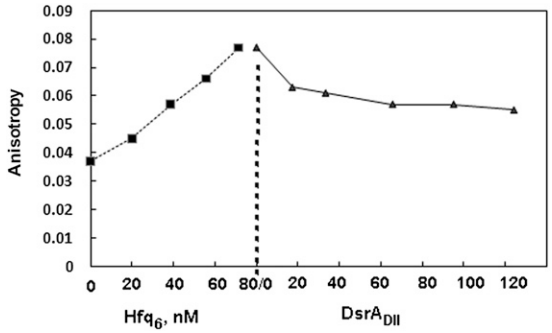

FIGURE 6. Fluorescence anisotropy experiment of FAM-A18 with Hfq and $DsrA_{DII}$. Hfq was titrated to 100 nM FAM-A_{18} to give 0.080, ~45% of the maximum anisotropy. Then aliquots of unlabeled $DsrA_{DII}$ were added to give the concentrations shown.

observe the expected anisotropy increase resulting from formation of a ternary complex. However the outcome was similar (data not shown). When Hfq and FAM-$DsrA_{DII}$ were preformed and A_{18} or polyA added to the solution, a similar decrease in anisotropy was observed (data not shown). The above results were surprising given the outcome of gel shift experiments (Brescia et al. 2003; Mikulecky et al. 2004; Updegrove et al. 2008) that clearly show complexes can form involving Hfq_6, DsrA, and a poly A sequence. The apparently disparate implications of the two types of experiments may, however, be reconcilable as discussed below.

DISCUSSION

The results from mass spectrometry, analytical ultracentrifugation, fluorescence anisotropy, and competition gel mobility shift assay all point to a 1:1 stoichiometry for the Hfq_6•A_{18} and Hfq_6•$DsrA_{DII}$ complexes. The more limited studies on Hfq binding to the RNAs DsrA, RprA, OxyS and OxyS-18 support a similar conclusion. These experiments were carried out with RNA concentrations from 4 nM to 5 μM in solvents with 0.1–0.5 M Na^+. The 1:1 stoichiometry is the same value determined by isothermal titration calorimetry measurements of Hfq_6 binding DsrA or a 140-nt *rpoS* mRNA segment (Mikulecky et al. 2004), but differs from the 2:1 (Hfq_6:RNA) stoichiometry inferred from gel shift assays of Hfq_6 binding to DsrA, a 138-nt *rpoS* RNA (Lease and Woodson 2004), $DsrA_{DII}$ (Sun and Wartell 2006), and RprA (Updegrove et al. 2008), as well as the fluorescence anisotropy and fluorescence quenching study of Hfq_6 binding to A_{18} (Sun and Wartell 2006). Since two methods used in the current work, mass spectrometry and sedimentation equilibrium, are robust model-independent approaches, our results raise the question why a 2:1 stoichiometry was inferred from previous investigations.

The results described by Figure 4a provide an explanation why a 2:1 stoichiometry was previously misinterpreted from the fluorescence anisotropy measurements of Hfq binding to FAM-A_{18} at low nanomolar concentrations. The anisotropy of the fully bound FAM-A_{18}, A_b, appears to have been previously underestimated. Increasing the experimentally derived value of A_b by ~11% produced a much better fit to the data using the 1:1 model. Assuming some flexibility in the A_b value can be justified since there is uncertainty in the Hfq_6 concentration required to saturate binding of FAM-A_{18}. With this adjustment to A_b, the difference between the predictions of the 2:1 model versus the 1:1 model no longer persuasively favors the 2:1 model.

The 2:1 stoichiometry inferred from the gel shift assay was suggested by equilibrium binding analyses of gel shift data obtained using 2–4 nM RNA that indicated a Hill coefficient above 2, as well as from data obtained with 400 nM to 1.0 μM of RNA, concentrations above the K_d (Lease and Woodson 2004; Sun and Wartell 2006). Since similar outcomes came from different laboratories, it seems unlikely that differences in binding activity of Hfq preparations influenced this outcome. Also, the Hfq used in the current experiments, which yield a 1:1 stoichiometry, reproduced the outcome of the gel shift assay (data not shown). While a definitive argument cannot yet be made why the gel shift assay yielded a 2:1 stoichiometry, several factors that might complicate interpretation of gel shift data may provide an explanation.

The equilibrium established in the sample solution may be altered as the low ionic strength buffer (0.5× TBE) exchanges with the loading buffer as the macromolecules enter the gel or during electrophoresis (Bloomfield et al. 2000). Although a low ionic strength solution may stabilize Hfq•RNA complexes, it has also been shown to produce well-ordered fibers of Hfq_6 (Arluison et al. 2006). If Hfq_6 aggregates in the gel environment it could alter the nature or amount of the Hfq•RNA complexes.

Factors governing the mass transport of Hfq•RNA complexes in a gel may also contribute to misleading interpretation of gel shift data, independent of the potential for Hfq_6 aggregation. Using a phenomenological theory of gel electrophoresis, Cann (1989) simulated the gel patterns produced by several protein–DNA interactions employing association and dissociation rate constants representative of the interactions and experimentally derived transport parameters. The simulations validated the application of the gel shift method for determining binding constants and stoichiometry for strong interactions with association (k_a) and dissociation (k_d) rate constants of $k_a = 3 \times 10^9$ $M^{-1}sec^{-1}$, $k_d = 1.3 \times 10^{-4}$ sec^{-1}. However the simulation also showed that a significant amount of the initial protein–nucleic acid complex entering the gel can irreversibly dissociate during electrophoresis. When parameters mimicking an intermediate strength complex were used ($k_a = 1.3 \times 10^6$ $M^{-1}sec^{-1}$, $k_d = 1.3 \times 10^{-4}$ sec^{-1}) with 10 nM each of protein and nucleic acid, 49% of the initial protein–nucleic acid complex irreversibly dissociated from this

band during electrophoresis. The extent of irreversible dissociation of the initial protein–nucleic acid complexes clearly depends on the concentrations used and the parameters of the system. The importance of these considerations has been demonstrated for properly interpreting gel shift data on a repressor-DNA operator system (Kleinschmidt et al. 1991).

It is worth noting that in the above example although electrophoresis depleted the amount of material in the nucleic acid–protein band, the unbound nucleic acid band could still be used to calculate the equilibrium dissociation constant to good accuracy (Cann 1989). Thus gel shift data can be used to evaluate binding constants, even when the nucleic acid–protein bands do not accurately reflect the initial amount of these complexes. We note that interpretation of the competition gel shift experiment described in Figure 3 does not depend on a quantitative evaluation of band intensities. The absence of a band intermediate between the shifted bands corresponding to RNA bound to wt-Hfq or Hfq-65 is consistent with 1:1 complexes.

The third method that suggested a 2:1 stoichiometry for Hfq_6•A_{18} was fluorescence quenching of Hfq's tyrosines by A_{18}. Quenching of Hfq fluorescence saturated when the amount of added A_{18} reached a molar ratio of 0.5:1 (A_{18}:Hfq_6) (Sun and Wartell 2006). Controls indicated that the inner filter effect (Lakowicz 2006) due to the absorbance of A_{18} at the excitation wavelength was negligible. We are currently unable to reconcile the apparent 2:1 stoichiometry implied from this experiment with the 1:1 stoichiometry determined in the current work. It is possible that A_{18} binding has a complex effect on the fluorescence of Hfq's three tyrosines such that a straightforward interpretation of the data is quantitatively flawed.

Several lines of evidence have shown that Hfq_6 possesses two distinct RNA binding surfaces (Mikulecky et al. 2004). The proximal surface appears to be involved in Hfq binding to a single-stranded sequence with several uracils and/or adenines adjacent to one or more hairpins (Schumacher et al. 2002; Zhang et al. 2002; Geissmann and Touati 2004). The distal surface of Hfq_6 binds to a repeated motif $(ARN)_n$, $n \geq 4$ (with R a purine, N any nucleoside) (Link et al. 2009). The latter motif includes the poly(A) sequence at the 3′ ends of mRNAs, and segments found in the 5′ leader region of at least two mRNAs (Soper and Woodson 2008; Salim and Feig 2010). With two distinct binding surfaces, a single Hfq hexamer has the potential to bind a mRNA and sRNA simultaneously.

The MALDI-TOF results suggest the existence of a Hfq_6•A_{18}•$DsrA_{DII}$ complex; however, the small size of the peak does not support the notion that a 1:1:1 complex is very stable. The fluorescence anisotropy experiment in Figure 6 also does not provide evidence for a stable ternary complex in solution. DsrA and A_{18} do not appear to bind Hfq independently under the conditions of the experiment. This appears to contradict the observation that polyA sequences can form a ternary complex with Hfq_6 and DsrA in polyacrylamide gels. A possible explanation of these observations may be related to the low ionic strength solvent and cage effect of the gel environment. Studies by de Haseth and Uhlenbeck (1980a) as well as the more recent demonstration of Hfq fibers (Arluison et al. 2006) indicate that low ionic strength solutions promote Hfq aggregation. The gel environment may promote Hfq_6 aggregation and enable ternary complexes that involve more than one Hfq_6. These complexes may not form in the 0.1 M Na^+ solution employed in the anisotropy experiment.

A counter hypothesis that can explain why putative ternary complexes are not reported by fluorescence anisotropy is more difficult. If the dissociation lifetime of a ternary complex is shorter than its rotational correlation time (τ_c) it could go undetected. For a 1:1:1 complex of DsrA, FAM-A_{18}, and Hfq_6, τ_c can be estimated to be ~60 nsec (Serdyuk et al. 2007). A dissociation lifetime this short is inconsistent with a stable ternary complex. The total anisotropy reflects the sum of each anisotropic species. Binding of $DsrA_{DII}$ or DsrA to FAM-A_{18}•Hfq_6 is expected to slow the rotational correlation time and increase anisotropy. If binding also induces a conformational change that partially releases the FAM –A_{18}, it may cancel the effect of the increased size on the rotational correlation time and in principle could reduce the anisotropy. In order to explain all of the results, this would also have to be true for A_{18} binding to $DsrA_{DII}$•Hfq_6. This seems a less likely explanation of the data than displacement of the bound RNA from Hfq_6 by the other RNA.

Regardless of the uncertainty and a definitive explanation for the stoichiometry reported by the previous gel results and the nature of the polyA-Hfq-DsrA complex observed in gels, the major conclusion from this work, that Hfq_6 has a 1:1 binding stoichiometry with RNA at concentration and ionic strength conditions mimicking a cell environment, addresses a question important to understanding how Hfq facilitates interactions between RNAs.

MATERIALS AND METHODS

Purification and characterization of wt and mutant Hfq

The Impact-CN intein system (New England Biolabs) was used to purify Hfq proteins as previously described (Sun and Wartell 2006). The plasmids used to overexpress the Hfq proteins contained the *E. coli hfq* gene inserted into SapI-SmaI–digested pTYB11 plasmid (pEcHfq) or mutant derivatives (see below). Protein purification was carried out according to the recommendation of the manufacturer using strain ER2566. Cell lysis was carried out using a French press. The cell lysate was centrifuged and the supernatant loaded onto a chitin column. The column was extensively washed with the lysis/wash buffer of 20 mM Tris (pH 8.3) and 1 M NaCl prior to incubation of the column with this buffer plus 40 mM dithiothreitol. The eluted protein was

concentrated and buffer-exchanged to 0.5 M NaCl and 20 mM Tris (pH 8.3) using centrifugation filtration units.

To remove contaminating nucleic acids, Hfq preparations were subjected to a micrococcal nuclease treatment. Twenty-five microliters of 300 U/mL micrococal nuclease (Worthington Biochemical) was added to 1 mL of 0.3–0.4 OD_{274nm} Hfq in 0.2 M NaCl, 20 mM Tris (pH 8.5), and 5 mM $CaCl_2$ and incubated for 45 min at 37°C. This nuclease has a strict dependence on Ca^{2+}. Ten microliters of 0.5 M Na_2EDTA was added, and sample was washed and concentrated in 15 mL of 0.5 M NaCl and 20 mM Tris (pH 8.3) using 30 kDa MWCO Amicon Utrafiltration cell.

The mutant Hfq protein, Hfq-65, was produced for this study from the plasmid pHfq-65, which was generated from pEcHfq using the QuikChange Mutagenesis Kit from Stratagene (Sun and Wartell 2006). Oligonucleotides employed placed a stop codon at position 66 of the *hfq* gene: 5′- GCGATTTCTACTGTTGTC CCGTCTTAGCCGGTTTCTCATCACAG-3′ and 5′-CTGTGATG AGAA ACCGGCTAAGACGGGAC AACAGTAGAAATCGC-3′. The plasmid construct was verified by DNA sequencing. The purification procedure for the mutant protein was similar to that used for wt Hfq. All proteins displayed expected molecular weights on a denaturing sodium dodecyl sulfate-polyacrylamide gel electrophoresis (SDS-PAGE). Concentrations were determined using an extinction coefficient of ϵ = 2900 M^{-1} cm^{-1} at 274 nm for the truncated protein and 4250 M^{-1} cm^{-1} for wt Hfq (Gill and von Hippel 1989). Ultraviolet spectra showed absorbance ratios of A_{275nm}/A_{255nm} (peak to valley) of ≥1.8. Analysis of the spectra indicated <5% contaminating nucleic acids (Sun and Wartell 2006).

RNA synthesis and purification

The following RNAs were purchased commercially (Integrated DNA Technologies) and purified by HPLC: $DsrA_{DII}$ (AACGA AUUUUUUAAGUGCUUCUUGCUUAAGCAAGUUUC), OxyS-18 (GAAUAACUAAAGCCAACG), and A_{18}. $DsrA_{DII}$ and A_{18} were also purchased with 6-carboxyfluorescein (FAM) linked to their 5′ end. The full-length DsrA, OxyS, and RprA RNAs were cloned as described previously and transcribed using a T7 MEGAscript High Yield RNA transcription kit (Ambion) (Updegrove et al. 2008). They were ^{32}P-labeled at their 5′ end using standard phosphatase and kinase reactions and purified by gel extraction (Sambrook and Russell 2001).

Mass spectrometry and cross-linking of Hfq to RNA

Twenty microliter samples were prepared by adding Hfq to fixed amounts of A_{18}, $DsrA_{DII}$, or OxyS-18 in phosphate binding buffer (0.2 M NaCl, 20 mM Na_2HPO_4 at pH 7.8). Concentrations are described in Results. For the Hfq-A_{18} mixture, 10 μL of 0.2 M EDC (1-ethyl-3-3-dimethylaminopropyl carbodiimide hydrochloride; Pierce) was added and allowed to react for 4 h at room temperature. For the other Hfq-RNA mixtures, 2 μL of a 3% formaldehyde solution was added and allowed to react for 15 min at room temperature. One microliter of 3 M glycine (in water) was then added to quench the reaction (Niranjanakumari et al. 2002). Twenty microliters of the Hfq-RNA solutions described above was then concentrated to 3 μL with a C4 ZipTip (Millipore) and then mixed with 3 μL of matrix solution. The matrix solution was prepared by adding 20 mg of sinapinic acid and 50 mg ammonium citrate in 500 μL of 18 MΩ deionized water. One microliter of analyte-matrix mixture was then deposited onto a 100-well stainless steel MALDI plate. The MALDI-MS experiments were performed using a Voyager DE STR MALDI-TOF mass spectrometer (Applied Biosystems) equipped with a 337-nm N_2 laser (3 Hz). The accelerating voltage, grid voltage, and delay time were typically 25 kV, 91%, and 1500 nsec, respectively. The laser intensity was checked daily to obtain the best signal-to-noise ratio. Mass spectra were obtained by averaging 10–50 laser shots.

Analytical ultracentrifugation

Sedimentation velocity

Sedimentation studies were performed in a Beckman Optima XLA analytical ultracentrifuge equipped with absorbance optics and an An60 Ti rotor at 19.7°C. Temperature was calibrated as described previously (Liu and Stafford 1995). Velocity data were typically collected at the appropriate speeds using 274 nm for Hfq and 495 nm for FAM-A_{18} at a spacing of 0.01 cm with one flash at each point in a continuous-scan mode. When collecting data at multiple wavelengths, care must be taken to collect data at peaks to avoid dramatic signal variations due to wavelength uncertainty (±4 nm) with the XLA. All experiments were initially analyzed with Sedfit to produce c(*s*) distributions (Schuck et al. 2002) and with $DCDT^{+2}$ to produce g(*s*) distributions and weight average S value (Philo 2006). Direct boundary fitting of velocity data to discrete models can also be performed with the program Sedanal (Stafford and Sherwood 2004). Analysis with Sedanal requires input of molecular weight, extinction coefficients, and density increments (typically estimated from 1-vbar*rho values). The buffer solution density was estimated in Sednterp to be 1.01920 gm/mL at 19.7°C. The vbar of Hfq was estimated with Sednterp (Laue et al. 1992) to be 0.7248. The vbar of FAM-A_{18} is assumed to be 0.55. The extinction coefficient of FAM-A_{18} at 495 nm is 75,000 $M^{-1}cm^{-1}$ or, using a molecular weight of 6113 Da, 12.269 mL/mg/cm. The extinction coefficient of Hfq at 274 nm is 0.400 mL/mg/cm (Stafford and Sherwood 2004). Parameter uncertainty is calculated with an Fstat routine within Sedanal at the 95% confidence interval and reported in a <, > format.

Sedimentation equilibrium

Hfq alone (at 2, 4, and 8 μM) or mixed at a 1:1 ratio with FAM-A_{18} was spun at 19.7°C and at 12K, 16K, and 20K in six-channel double sector cells. Data on Hfq alone were collected at 274 nm. Data with mixtures of Hfq and FAM-A_{18} were collected at 495 nm. Equilibrium at each speed was judged with the software utility WinMATCH (http://www.biotech.uconn.edu/auf/?i=aufftp). This program makes a least-square comparison of successive scans to establish that equilibrium has been achieved. Values for density, vbar, and extinction coefficients were as described under Sedimentation Velocity. Nine data sets from three concentrations and three speeds were best fit to a single species model using Sedanal. Molecular weight uncertainty is calculated with Fstat as described above.

Polyacrylamide gel electrophoresis

Gel mobility shift assay

Binding reactions of Hfq and FAM-A_{18} were carried out in the phosphate binding buffer (0.2 M NaCl, 20 mM Na_2HPO_4 at pH 7.8). wt Hfq, Hfq-65, or both were added to FAM-A_{18} and the

reactions allowed to equilibrate at 25°C for 10 min prior to the addition of 3.2 μL of gel loading buffer (100 mM Tris-Cl at pH 6.8, 4% [w/v] SDS, 0.2% [w/v] bromophenol blue, 20% [v/v] glycerol). Final reaction volumes were 20 μL and contained 0.6% SDS. The SDS was added in order to enhance the negative charge of the Hfq•A_{18} complexes and enable them to migrate into the gel prior to the free A_{18} running out the bottom. The concentration of Hfq (moles hexamer) in each reaction varied between 2 and 3 μM, and the concentration of FAM-A_{18} was 1 μM. The total reaction volumes were electrophoresed into a 6% polyacrylamide (29:1) gel with 4% glycerol that was layered onto a 2.5-cm bottom plug consisting of 15% polyacrylamide (29:1). The latter was employed to slow and retain the free A_{18}. The gel was 20 cm × 20 cm × 1.5 mm. Electrophoresis was conducted at 120 V at 4°C using 1× TBE buffer for ~8 h. Analysis of the gels used excitation and emission wavelengths of 473 and 520 nm, respectively, of the Fujifilm Image Reader FLA-3000.

Similar competition gel assays were carried out in which wt Hfq, Hfq-65, or both were bound with ^{32}P-labeled DsrA, RprA, or OxyS in 15 μL binding solution (50 mM NaCl, 50 mM KCl, 100 mM NH_4Cl, 20 mM Tris-HCl at pH 8.0, 4% glycerol). The indicated amounts of Hfq were added to the indicated amount of sRNA and the reaction allowed to equilibrate for 10 min at 25°C prior to running on a 8% polyacrylamide (29:1) gel with 3% glycerol. Electrophoresis was conducted at 120 V at 4°C using 1× TBE buffer for ~2 h. Imaging and analysis of the gels were made using the Fujifilm Image Reader FLA-3000.

Fluorescence anisotropy measurements

Fluorescence anisotropy measurements of Hfq binding to FAM-A_{18} were carried out at room temperature in the 0.5 M NaCl and 20 mM Tris (pH 8.3) solvent as previously described (Sun and Wartell 2006). The L-format was employed with the excitation monochromator at 490 nm and emission monochromator at 522 nm. Anisotropy values were obtained from the average of 10 iterations using an integration time of 4–8 sec for each measurement depending on FAM-A_{18} concentration. The slits employed were set at 1 or 2 mm. wt Hfq was serially titrated into fluorescence cells with a working volume of 1 mL or 0.5 mL for FAM-A_{18} at 2 nM. When 5 μM of FAM-A_{18} was employed, a 50 μL micro-cell was employed. The fluorescence intensity of FAM-A_{18} showed a small decrease with Hfq binding after accounting for dilution (~2%). Similar anisotropy experiments were carried using $DsrA_{DII}$ with FAM attached to its 5′ end. The solvent employed for the FAM-$DsrA_{DII}$ experiments was 0.1 M NaCl and 20 mM Tris (8.3) since Hfq affinity for $DsrA_{DII}$ increased with decreasing salt concentration and conditions favoring strong binding were sought (data not shown). Unlike FAM-A_{18}, Hfq binding decreased the fluorescence intensity of FAM-$DsrA_{DII}$, indicating that the quantum yield of the bound fluorophore was less than the free molecule. The ratio of quantum yield for bound versus free FAM-$DsrA_{DII}$, Q_b/Q_f, was determined to be 0.70 by saturating FAM-$DsrA_{DII}$. The change in anisotropy was corrected for this factor (Lundblad et al. 1996).

Analysis of fluorescence anisotropy data

The two models employed in the analysis of Hfq binding to FAM-A_{18} at low concentration (nM) were described by Sun and Wartell (2006). Both assume that Hfq exists only as hexamers. The first model assumes a one-to-one complex forms between the Hfq hexamer and FAM-A_{18}. An equation describing the fluorescence anisotropy in terms of the dissociation constant K_d and other parameters of the experiment can be derived (Lundblad et al. 1996) and is given by Equation 1.

$$A = A_f + (A_b - A_f)\,[\beta - (\beta^2 - 4R_tP_t)^{1/2}]/2R_t, \qquad (1)$$

where $\beta = R_t + P_t + K_d$. A is the measured anisotropy of FAM-A_{18} during the titration; A_f and A_b are the anisotropy of the free and bound FAM-A_{18} respectively; and R_t and P_t are the total concentrations of FAM-A_{18} and Hfq hexamer respectively. Nonlinear least-squares fit of the equation to data was made. For a situation where binding quenches the fluorescence of the RNA (i.e., $DsrA_{DII}$), Equation 1 has to be corrected for the difference in quantum yields for free and bound RNA (Q_f, Q_b). Defining $\alpha = [\beta - [\beta^2 - 4\,R_t\,P_t]^{1/2}]/2R_t$ one obtains

$$A = [A_f + (A_b\,(Q_b/Q_f) - A_f)\alpha]/[1 - (1 - (Q_b/Q_f))\alpha]. \qquad (2)$$

The second model assumed that Hfq hexamers bind FAM-A_{18} in a two-step reaction. The binding reaction is described by a dissociation constant K_1 for binding the first Hfq hexamer, and a dissociation constant K_2 for binding a subsequent Hfq hexamer:

$$R + P \quad \leftrightarrow \quad RP \text{ with } K_1 = (R)(P)/RP \qquad (3a)$$

$$RP + P \quad \leftrightarrow \quad RP_2 \text{ with } K_2 = (RP)(P)/RP_2. \qquad (3b)$$

P corresponds to Hfq hexamer and R is FAM-A_{18}. Data were fit to the second model using the BIOEQS program (Royer and Beechem 1992; Royer 1993). This algorithm performs a nonlinear least-squares fit of Equation 3 to the anisotropy data using parameters corresponding to the standard state free energies related to K_1 and K_2, anisotropies of free RNA, RNA in the RP complex, and RNA in the RP_2 complex. The anisotropy of the free FAM-A_{18} was fixed to the experimental value, and the remaining four parameters fit to the data. Supplementary information for Figures S1 to S3 is available upon request.

SUPPLEMENTAL MATERIAL

Supplemental material is available for this article.

ACKNOWLEDGMENTS

We were supported by a Georgia Tech/CDC seed grant and funding from the NASA Astrobiology Institute as well as a URS award to C.T. by the Institute of Bioengineering and Biosciences.

Received September 8, 2010; accepted November 24, 2010.

REFERENCES

Arluison V, Mura C, Guzman MR, Liquier J, Pellegrini O, Gingery M, Regnier P, Marco S. 2006. Three-dimensional structures of fibrillar Sm proteins: Hfq and other Sm-like proteins. *J Mol Biol* **356:** 86–96.

Arluison V, Hohng S, Roy R, Pellegrini O, Regnier P, Ha T. 2007. Spectroscopic observation of RNA chaperone activities of Hfq in post-transcriptional regulation by a small non-coding RNA. *Nucleic Acids Res* **35:** 999–1006.

Azam TA, Hiraga S, Ishihama A. 2000. Two types of localization of the DNA-binding proteins within the *Escherichia coli* nucleoid. *Genes Cells* **5:** 613–626.

Bloomfield VA, Crothers DM, Tinoco I. 2000. *Nucleic acids: Structures, properties, and functions*. University Science Books, Sausalito, CA.

Brennan RG, Link TM. 2007. Hfq structure, function and ligand binding. *Curr Opin Microbiol* **10:** 125–133.

Brescia CC, Mikulecky PJ, Feig AL, Sledjeski DD. 2003. Identification of the Hfq-binding site on DsrA RNA: Hfq binds without altering DsrA secondary structure. *RNA* **9:** 33–43.

Butland G, Peregrin-Alvarez JM, Li J, Yang W, Yang X, Canadien V, Starostine A, Richards D, Beattie B, Krogan N, et al. 2005. Interaction network containing conserved and essential protein complexes in *Escherichia coli*. *Nature* **433:** 531–537.

Cann JR. 1989. Phenomenological theory of gel electrophoresis of protein-nucleic acid complexes. *J Biol Chem* **264:** 17032–17040.

Carmichael GG, Weber K, Niveleau A, Wahba AJ. 1975. The host factor required for RNA phage Qbeta RNA replication in vitro. Intracellular location, quantitation, and purification by polyadenylate-cellulose chromatography. *J Biol Chem* **250:** 3607–3612.

Cunning C, Brown L, Elliott T. 1998. Promoter substitution and deletion analysis of upstream region required for rpoS translational regulation. *J Bacteriol* **180:** 4564–4570.

de Haseth PL, Uhlenbeck OC. 1980a. Interaction of *Escherichia coli* host factor protein with oligoriboadenylates. *Biochemistry* **19:** 6138–6146.

de Haseth PL, Uhlenbeck OC. 1980b. Interaction of *Escherichia coli* host factor protein with Q beta ribonucleic acid. *Biochemistry* **19:** 6146–6151.

Folichon M, Arluison V, Pellegrini O, Huntzinger E, Regnier P, Hajnsdorf E. 2003. The poly(A) binding protein Hfq protects RNA from RNase E and exoribonucleolytic degradation. *Nucleic Acids Res* **31:** 7302–7310.

Folichon M, Allemand F, Regnier P, Hajnsdorf E. 2005. Stimulation of poly(A) synthesis by *Escherichia coli* poly(A)polymerase I is correlated with Hfq binding to poly(A) tails. *FEBS J* **272:** 454–463.

Geissmann TA, Touati D. 2004. Hfq, a new chaperoning role: Binding to messenger RNA determines access for small RNA regulator. *EMBO J* **23:** 396–405.

Gill SC, von Hippel PH. 1989. Calculation of protein extinction coefficients from amino acid sequence data. *Anal Biochem* **182:** 319–326.

Karas M, Gluckmann M, Schafer J. 2000. Ionization in matrix-assisted laser desorption/ionization: Singly charged molecular ions are the lucky survivors. *J Mass Spectrom* **35:** 1–12.

Kawamoto H, Koide Y, Morita T, Aiba H. 2006. Base-pairing requirement for RNA silencing by a bacterial small RNA and acceleration of duplex formation by Hfq. *Mol Microbiol* **61:** 1013–1022.

Kleinschmidt C, Tovar K, Hillen W. 1991. Computer simulations and experimental studies of gel mobility patterns for weak and strong non-cooperative protein binding to two targets on the same DNA: Application to binding of tet repressor variants to multiple and single tet operator sites. *Nucleic Acids Res* **19:** 1021–1028.

Lakowicz JR. 2006. *Principles of fluorescence spectroscopy*. Springer, New York.

Laue TM, Shah B.D., Ridgeway, T.M. and Pelletier, S.L. 1992. *Analytical ultracentrifugation in biochemistry and polymer sciences*. (ed. SE Harding, et al.) Royal Society of Chemistry, Cambridge, UK.

Le Derout J, Folichon M, Briani F, Deho G, Regnier P, Hajnsdorf E. 2003. Hfq affects the length and the frequency of short oligo(A) tails at the 3′ end of *Escherichia coli* rpsO mRNAs. *Nucleic Acids Res* **31:** 4017–4023.

Le Derout J, Boni IV, Regnier P, Hajnsdorf E. 2010. Hfq affects mRNA levels independently of degradation. *BMC Mol Biol* **11:** 17.

Lease RA, Woodson SA. 2004. Cycling of the Sm-like protein Hfq on the DsrA small regulatory RNA. *J Mol Biol* **344:** 1211–1223.

Lenz DH, Mok KC, Lilley BN, Kulkarni RV, Wingreen NS, Bassler BL. 2004. The small RNA chaperone Hfq and multiple small RNAs control quorum sensing in Vibrio harveyi and Vibrio cholerae. *Cell* **118:** 69–82.

Link TM, Valentin-Hansen P, Brennan RG. 2009. Structure of *Escherichia coli* Hfq bound to polyriboadenylate RNA. *Proc Natl Acad Sci* **106:** 19292–19297.

Liu S, Stafford WF III. 1995. An optical thermometer for direct measurement of cell temperature in the Beckman instruments XL-A analytical ultracentrifuge. *Anal Biochem* **224:** 199–202.

Lundblad JR, Laurance M, Goodman RH. 1996. Fluorescence polarization analysis of protein-DNA and protein-protein interactions. *Mol Endocrinol* **10:** 607–612.

Majdalani N, Hernandez D, Gottesman S. 2002. Regulation and mode of action of the second small RNA activator of RpoS translation, RprA. *Mol Microbiol* **46:** 813–826.

Majdalani N, Vanderpool CK, Gottesman S. 2005. Bacterial small RNA regulators. *Crit Rev Biochem Mol Biol* **40:** 93–113.

Masse E, Escorcia FE, Gottesman S. 2003. Coupled degradation of a small regulatory RNA and its mRNA targets in Escherichia coli. *Genes Dev* **17:** 2374–2383.

Mikulecky PJ, Kaw MK, Brescia CC, Takach JJ, Sledjeski D, Feig AL. 2004. *Escherichia coli* Hfq has distinct interaction surfaces for DsrA, rpoS and poly(A) RNAs. *Nat Struct Mol Biol* **11:** 1206–1214.

Mohanty BK, Kushner SR. 2006. The majority of *Escherichia coli* mRNAs undergo post-transcriptional modification in exponentially growing cells. *Nucleic Acids Res* **34:** 5695–5704.

Mohanty BK, Maples VF, Kushner SR. 2004. The Sm-like protein Hfq regulates polyadenylation dependent mRNA decay in *Escherichia coli*. *Mol Microbiol* **54:** 905–920.

Moller T, Franch T, Hojrup P, Keene DR, Bachinger HP, Brennan RG, Valentin-Hansen P. 2002a. Hfq: A bacterial Sm-like protein that mediates RNA-RNA interaction. *Mol Cell* **9:** 23–30.

Moller T, Franch T, Udesen C, Gerdes K, Valentin-Hansen P. 2002b. Spot 42 RNA mediates discoordinate expression of the *E. coli* galactose operon. *Genes Dev* **16:** 1696–1706.

Morita T, Maki K, Aiba H. 2005. RNase E-based ribonucleoprotein complexes: Mechanical basis of mRNA destabilization mediated by bacterial noncoding RNAs. *Genes Dev* **19:** 2176–2186.

Niranjanakumari S, Lasda E, Brazas R, Garcia-Blanco MA. 2002. Reversible cross-linking combined with immunoprecipitation to study RNA-protein interactions in vivo. *Methods* **26:** 182–190.

Philo JS. 2006. Improved methods for fitting sedimentation coefficient distributions derived by time-derivative techniques. *Anal Biochem* **354:** 238–246.

Royer CA. 1993. Improvements in the numerical analysis of thermodynamic data from biomolecular complexes. *Anal Biochem* **210:** 91–97.

Royer CA, Beechem JM. 1992. Numerical analysis of binding data: Advantages, practical aspects, and implications. *Methods Enzymol* **210:** 481–505.

Salim NN, Feig AL. 2010. An upstream Hfq binding site in the fhlA mRNA leader region facilitates the OxyS-fhlA interaction. *PLoS ONE* **5:** e13029. doi: 10.1371/journal.pone.0013028.

Sambrook J, Russell DW. 2001. *Molecular cloning: A laboratory manual*. Cold Spring Harbor Laboratory Press, Cold Spring Harbor, NY.

Schuck P, Perugini MA, Gonzales NR, Howlett GJ, Schubert D. 2002. Size-distribution analysis of proteins by analytical ultracentrifugation: Strategies and application to model systems. *Biophys J* **82:** 1096–1111.

Schumacher MA, Pearson RF, Moller T, Valentin-Hansen P, Brennan RG. 2002. Structures of the pleiotropic translational regulator Hfq and an Hfq-RNA complex: A bacterial Sm-like protein. *EMBO J* **21:** 3546–3556.

Serdyuk IN, Zaccai NR, Zaccai G. 2007. *Methods in molecular biophysics: Structure, dynamics, function*. Cambridge University Press, Cambridge.

Sledjeski DD, Whitman C, Zhang A. 2001. Hfq is necessary for regulation by the untranslated RNA DsrA. *J Bacteriol* **183:** 1997–2005.

Soper TJ, Woodson SA. 2008. The rpoS mRNA leader recruits Hfq to facilitate annealing with DsrA sRNA. *RNA* **14:** 1907–1917.

Stafford WF, Sherwood PJ. 2004. Analysis of heterologous interacting systems by sedimentation velocity: Curve fitting algorithms for estimation of sedimentation coefficients, equilibrium and kinetic constants. *Biophys Chem* **108:** 231–243.

Steege DA. 2000. Emerging features of mRNA decay in bacteria. *RNA* **6:** 1079–1090.

Sun X, Wartell RM. 2006. *Escherichia coli* Hfq binds A18 and DsrA domain II with similar 2:1 Hfq6/RNA stoichiometry using different surface sites. *Biochemistry* **45:** 4875–4887.

Takada A, Wachi M, Kaidow A, Takamura M, Nagai K. 1997. DNA binding properties of the hfq gene product of *Escherichia coli*. *Biochem Biophys Res Commun* **236:** 576–579.

Tsui HC, Feng G, Winkler ME. 1997. Negative regulation of mutS and mutH repair gene expression by the Hfq and RpoS global regulators of *Escherichia coli* K-12. *J Bacteriol* **179:** 7476–7487.

Updegrove T, Wilf N, Sun X, Wartell RM. 2008. Effect of Hfq on RprA-rpoS mRNA pairing: Hfq-RNA binding and the influence of the 5′ rpoS mRNA leader region. *Biochemistry* **47:** 11184–11195.

Updegrove TB, Correia JJ, Galletto R, Bujalowski W, Wartell RM. 2010. *E. coli* DNA associated with isolated Hfq interacts with Hfq's distal surface and C-terminal domain. *Biochim Biophys Acta* **1799:** 588–596.

Valentin-Hansen P, Eriksen M, Udesen C. 2004. The bacterial Sm-like protein Hfq: a key player in RNA transactions. *Mol Microbiol* **51:** 1525–1533.

Vecerek B, Rajkowitsch L, Sonnleitner E, Schroeder R, Blasi U. 2008. The C-terminal domain of *Escherichia coli* Hfq is required for regulation. *Nucleic Acids Res* **36:** 133–143.

Vytvytska O, Jakobsen JS, Balcunaite G, Andersen JS, Baccarini M, von Gabain A. 1998. Host factor I, Hfq, binds to *Escherichia coli* ompA mRNA in a growth rate-dependent fashion and regulates its stability. *Proc Natl Acad Sci* **95:** 14118–14123.

Waters LS, Storz G. 2009. Regulatory RNAs in bacteria. *Cell* **136:** 615–628.

Zhang A, Wassarman KM, Ortega J, Steven AC, Storz G. 2002. The Sm-like Hfq protein increases OxyS RNA interaction with target mRNAs. *Mol Cell* **9:** 11–22.